Specific Adhesion of Vesicles Monitored by Scanning Force Microscopy and Quartz Crystal Microbalance

Bruno Pignataro,* Claudia Steinem†, Hans-Joachim Galla,† Harald Fuchs,* and Andreas Janshoff*
*Physikalisches Institut, Westfälische Wilhelms-Universität, Wilhelm-Klemm-Str. 10, and †Institut für Biochemie, Westfälische Wilhelms-Universität, Wilhelm-Klemm-Str. 2, 48149 Münster, Germany

ABSTRACT The specific adhesion of unilamellar vesicles with an average diameter of 100 nm on functionalized surfaces mediated by molecular recognition was investigated in detail. Two complementary techniques, scanning force microscopy (SFM) and quartz crystal microbalance (QCM) were used to study adhesion of liposomes consisting of 1,2-dipalmitoyl-*sn*-glycero-3-phosphocholine and varying concentrations of *N*-((6-biotinoyl)amino)hexanoyl)-1,2-dihexadecanoyl-*sn*-glycero-3-phosphoethanolamine (biotin-X-DHPE). Monitoring the adhesion of the receptor-doped vesicles to avidin-coated gold surfaces by QCM (f_0 = 5 MHz) revealed an increased shift in resonance frequency with increasing biotin concentration up to 10 mol% biotin-X-DHPE. To address the question of how the morphology of the liposomes changes upon adhesion and how that contributes to the resonator's frequency response, we performed a detailed analysis of the liposome morphology by SFM. We found that, with increasing biotin-concentration, the height of the liposomes decreases considerably up to the point where vesicle rupture occurs. Thus, we conclude that the unexpected high frequency shifts of the quartz crystal (>500 Hz) can be attributed to a firm attachment of the spread bilayers, in which the number of contacts is responsible for the signal. These findings are compared with one of our recent studies on cell adhesion monitored by QCM.

INTRODUCTION

Cell–substrate and cell–cell interactions are among the most fundamental and interesting subjects in biophysical and biomedical research involving whole cells (Bongrand, 1995). Comprehensive understanding and control of cell spreading and growth on biocompatible materials is a prerequisite for successful cell culture (Cooper et al., 1995; Ruardy et al., 1997; Pignataro et al., 1997). The process of cell adhesion on artificial surfaces is a rather complex and versatile process involving different kinds of interactions (Gallez, 1994). A key role is played by molecular recognition between cell adhesion proteins anchored in the basal membrane and extracellular matrix proteins covering the substrate. At least two groups of proteins are involved in the interaction with surfaces: Integrins and proteoglycans. Questions arise like, what is the role of the cytoskeleton in cell adhesion, how strong are the bonds, which interaction dominates the adhesion process, and how do cells migrate and roll.

Due to the complex nature of this problem, research has been focused on suitable model systems for the study of isolated processes. Unilamellar vesicles in a wide size range (50 nm–20 μm) have been proven to be an excellent model to mimic cell adhesion in a protein-free environment (Albersdörfer et al., 1997, 1998). Considerable effort has been spent on the theoretical and experimental exploration of the adhesion of spherical vesicles on surfaces. A theoretical framework based on the elastic behavior of shells is available, providing the possibility to calculate the shape of vesicles on surfaces by numerically solving the corresponding Euler–Lagrange equations. The liposome shape generally depends on adhesion energy, external pressure, and bending rigidity of the membrane (Seifert, 1991; Seifert and Lipowski, 1995).

Research on the adhesion and rupture of vesicles on surfaces is also directed toward the development of solid-supported membranes serving as matrices for biosensors and stable model systems mimiking planar cell membranes. Preparation of solid-supported membranes can be accomplished by Langmuir–Blodgett films, detergent dilution (Terrettaz et al., 1993), and fusion of vesicles (Plant et al., 1994; Kalb et al., 1992); the latter is the easiest and most versatile method. However, basic research on the spreading mechanism is rare and preparation is a matter of trial and error.

Here, we present a study in which we used SFM (Binnig et al., 1986) and QCM (Buttry and Ward, 1992) techniques to investigate the adhesion of functionalized vesicles adsorbing specifically to surfaces by means of molecular recognition events. Both methods have been proven to be excellent tools to characterize biological membranes and associated processes in situ, revealing integral and spatially resolved information about surface features (Janshoff et al., 1996; Müller et al., 1997b; Schabert and Engel, 1995; Shao and Yang, 1995). SFM is the only technique to date that is capable of visualizing small liposomes in a natural environment. Besides topographic information, elastic properties of

Received for publication 20 July 1999 and in final form 20 October 1999.
Address reprint requests to Andreas Janshoff, Physikalisches Institut, Wilhelm-Klemm-Str. 10, 48149 Münster, Germany. Tel.: +49-251-83-39111; Fax: +49-251-83-33602; E-mail: janshof@nwz.uni-muenster.de.

Abbreviations used: SFM, scanning force microscopy; DPPC, 1,2-dipalmitoyl-*sn*-glycero-3-phosphocholine; biotin-X-DHPE, *N*-((6-biotinoyl)-amino)hexanoyl)-1,2-dihexadecanoyl-*sn*-glycero-3-phosphoethanolamine; RMS, root mean square; QCM, quartz crystal microbalance.

0006-3495/00/01/487/12 $2.00

the bilayer structures can be explored as demonstrated by Laney et al. (1997).

In this study, unilamellar vesicles of DPPC doped with various amounts of biotin-X-DHPE were used to study their binding to avidin/streptavidin-covered surfaces. The objective of the present work was twofold. First, we attempted to describe the spreading of the vesicles to garner insight into the change of vesicle morphology as a function of adhesion energy governed by adjustment of the lipid composition. The formation of planar bilayers on solid substrates due to vesicle-rupture at critical adhesion energy was visualized by SFM. The second issue addressed by this paper is a critical consideration of the used methods with emphasis on the explanation of the frequency response. Although the QCM technique is used in many fields of biophysical research and biosensor development, little is known about the effects, which determine the frequency response on adsorption of proteins, nucleic acids, cells, and liposomes. The most prominent candidates responsible for the deviation from Sauerbrey's (1959) equation are currently viscoelasticity of the biomaterial and the change of surface properties such as roughness, hydropathicity, polarity, and surface charge. We could demonstrate that the frequency shift observed by liposome adhesion is largely due to the contact area of the basal bilayer rather than to the viscoelastic body of the liposome. This has considerable consequences for data interpretation of cell adhesion on quartz resonators.

MATERIALS AND METHODS

Vesicle preparation

Vesicles were prepared from mixtures of DPPC and biotin-X-DHPE (Avanti, Alabaster, AL), in molar ratios of 99:1, 95:5, 90:10, 80:20, and 70:30. Mixed lipid films were prepared by drying the lipids dissolved in chloroform under a stream of nitrogen while heating above the main phase transition temperature of DPPC (T_m = 41.5°C) followed by 2 h under vacuum. Multilamellar vesicles were prepared by first swelling the lipid films in aqueous solution while heating above T_m and then vortexing periodically for 30 s. The resulting multilamellar vesicles were subsequently sized by a miniextruder (LiposoFast, Avestin, Ottawa, Canada) through polycarbonate membranes with 100-nm nominal pore diameters above T_m resulting in large unilamellar vesicles (LUVs). LUVs were suspended in buffer (10 mM TRIS/HCl, 20 mM NaCl, pH 7.4 for SFM and 10 mM TRIS/HCl, 20 mM NaCl, pH 8.0 for QCM measurements) at different lipid concentrations.

Surface functionalization and QCM setup

Plano–plano AT-cut quartz plates (14 mm in diameter) with a 5-MHz fundamental resonance frequency (KVG, Neckarbischofsheim, Germany) were coated with gold electrodes on both sides, each exhibiting an area of 0.33 cm^2. The quartz resonator was placed in a crystal holder made of Teflon, exposing one side of the resonator plate to the aqueous solution. Equipped with an inlet and outlet that connects the crystal holder to a peristaltic pump, the setup allows adding proteins and vesicles from outside the Teflon chamber. Electrical contact of the quartz plate with the oscillator circuit (SN74LS124N, Texas Instruments, Dallas, TX) was ensured by gluing copper wires to the gold surfaces using a silver adhesive. The entire system was placed in a water-jacketed chamber thermostatted at 20°C. The frequency change of the quartz resonator was recorded using a frequency counter (HP 53181A, Hewlett Packard, Palo Alto, CA) connected via RS 232 to a PC (Janshoff et al., 1996).

The freshly evaporated gold surfaces of the quartz plates were first cleaned in an argon plasma cleaner for 10 min (Plasma Cleaner, Harrick, New York, NY) before incubation in a 1-mM solution of 3-mercaptopropionic acid in ultrapure water for 30 min. Successful chemisorption was checked by contact angle measurements and impedance spectroscopy as reported previously (Steinem et al., 1997). The quartz plate mounted in the Teflon cell was rinsed thoroughly with buffer (10 mM TRIS/HCl, 20 mM NaCl, pH 8.0) and then placed in the thermostatted chamber at a constant buffer flow of 0.2 ml/min. Avidin was deposited by first dissolving the protein in the same buffer and then adding it to a vial connected to the quartz chamber by Teflon tubes. The final avidin concentration was 1.5 μM.

Surface functionalization and SFM imaging

SFM was performed using a Multimode/Nanoscope IIIa (Digital Instruments, Santa Barbara, CA). Protein layers and vesicles were imaged in contact mode at room temperature. A Teflon plate with a small mica sheet mounted in the center was used as the liquid cell. A droplet of buffer remains on the mica sheet due to the low surface tension of the surrounding Teflon (entrapped droplet technique). Commercially available silicon nitride tips (Park Instruments, Sunnyvale, CA) with a pyramidal shape were used. The spring constants of the cantilevers were determined by the thermal noise method (Hutter and Bechhoefer, 1993). Typical spring constants were around (0.01 $\pm$ 0.003) N/m. Imaging was performed at a scan rate of 0.8 Hz with a typical load force of 100 pN. To control the load force during imaging, we recorded force versus distance curves at the beginning and end of each image and accounted for the drift during imaging. Tip characteristics were estimated before imaging from scanning electron micrographs and test structures. Typical tip curvature radii and wall slopes were (50 $\pm$ 20) nm and 35°, respectively. Protein layers in air were imaged in TappingMode (Digital Instruments, Santa Barbara, CA) to obtain better resolution using etched silicon tips with an average tip radius of 10 nm.

The functionalization of the mica surfaces was performed by incubating freshly cleaved mica sheets ($\sim 3 \times 3$ mm^2) in a 1-mg/ml biotinylated bovine serum albumin (BBSA) solution (carrying ~8 biotins per protein) for 20 min. After rinsing with buffer (10 mM TRIS/HCl, 20 mM NaCl, pH 7.4), the pretreated surfaces were incubated in a streptavidin solution (0.1 mg/ml) for 30 min. Finally, the samples were thoroughly rinsed with buffer and incubated in the vesicle suspension (0.01–0.1 mg/ml) for 20 min followed by a buffer rinse.

RESULTS

QCM analysis of avidin adsorption on self-assembly films of 3-mercaptopropionic acid

The quartz crystal microbalance technique is a versatile method for in situ quantification of protein-, lipid-, and DNA-adsorption on functionalized surfaces. A prerequisite for the investigation of biotin-doped vesicle adsorption is a complete surface coverage with avidin serving as the receptor matrix. Avidin has a pI of 10–11 and can therefore be readily immobilized on negatively charged surfaces at slightly basic pH, which renders it a better choice than streptavidin in this particular case. To realize immobilization of avidin, we chose 3-mercaptopropionic acid mono-

layers self assembled on gold surfaces, which are negatively charged at pH 8.0 (pK_a 5.6). Figure 1 shows the observed frequency shift (Δf_{max} = (50 ± 5) Hz) after exposing the resonator to an avidin solution with a final concentration of 1.5 μM. This frequency shift is indicative of an avidin monolayer and essentially identical to the resonator's response upon adsorption of a streptavidin or avidin monolayer on a biotin functionalized surface. Adding more avidin did not alter the frequency, indicating that the surface is covered at its maximum. After incubation for 1 h, the quartz surface was rinsed thoroughly for 1 h to remove nonbound and loosely attached avidin before starting the experiment on vesicle adhesion. To verify that the binding capabilities of the immobilized avidin are preserved, we assayed the adsorption of BSA versus BBSA, in which only addition of BBSA resulted in a frequency decrease of (32 ± 2) Hz, representing a protein monolayer as deduced from fitting parameters of a Langmuir-type isotherm to the data (data not shown). Formation of alternating avidin/BBSA multilayers further confirmed preservation of their binding capability. It is noteworthy that both proteins, although bearing approximately the same molecular mass, exhibit different frequency responses in solution. It has been shown that Sauerbrey's equation, assuming a rigid mass attached to the resonator surface, applies only in a few cases concerning dry biomaterials and a shear resonator operating in air. In fact, the deviation from Sauerbrey's equation can be considerably large (Steinem et al., 1998; Wegener et al., 1998). Effects including viscoelastic properties of the adsorbed material, entrapped water, enhanced roughness, and charge distributions (Gouy–Chapmann layer) are discussed in this respect (Yang and Thompson, 1993a,b).

Adhesion of biotinylated vesicles on avidin monolayers monitored by QCM

The frequency change of the QCM in response to the adhesion of vesicles with various amounts of biotin-X-DHPE was investigated. The biotin-X-DHPE-doped LUVs with a diameter of 80–120 nm, which was estimated by light scattering experiments, were added to the avidin functionalized surface at 20°C while recording the resonant frequency. After addition of liposomes, the solution was first pumped through the quartz chamber for 10 min before stopping the flow. The response of the quartz crystal to the liposome adsorption was monitored for 180 min under "stand by" conditions before starting to rinse with buffer under continuous flow. Generally, it took (800 ± 200) s after stopping the buffer flow before the resonance frequency started to decrease, indicating that adsorption of the liposomes was taking place (Fig. 2 *A*). For better clarity, all frequency time traces were set to the time at which the frequency started to decrease. The frequency versus time traces depend on the biotin-X-DHPE amount in the vesicles. Figure 2 *B* shows the frequency shift due to adsorption of vesicles doped with various biotin-X-DHPE concentrations

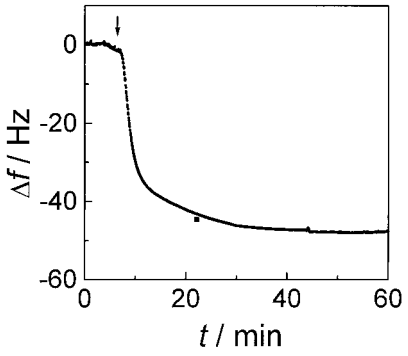

FIGURE 1 Representative time-dependent frequency trace showing the adsorption of avidin to a 3-mercaptopropionic acid monolayer chemisorbed on gold. The arrow indicates the injection time of the avidin solution (1.5 μM). The experiment was performed at 20°C in a buffer composed of 10 mM TRIS/HCl, 20 mM NaCl, pH 8.0.

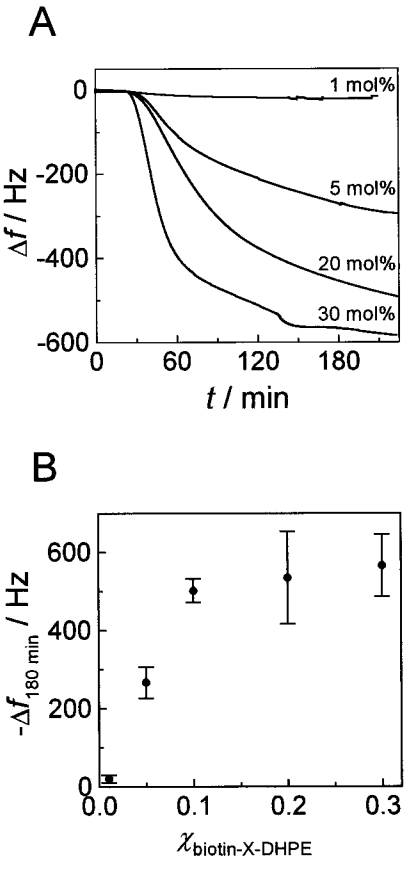

FIGURE 2 (*A*) Time-dependent frequency traces showing the adsorption of liposomes doped with different amounts of biotin-X-DHPE on an avidin layer. The injection time of the liposomes leading to a final lipid concentration of 0.3 mg/ml is indicated by $t = 0$. The buffer flow was stopped after 10 min. After 180 min, the cell was rinsed with buffer. The experiments were performed at 20°C in a buffer composed of 10 mM TRIS/HCL, 20 mM NaCl, pH 8.0. (*B*) Frequency decrease ($\Delta f = f - f_0$) after 3 h after liposome addition. All experiments were done twice, the errors are the mean error of the data.

after 180 min. Liposomes containing 1 mol% biotin-X-DHPE show a frequency decrease of only 20 Hz. However, increasing the biotin concentration up to 10–30 mol% led to a decrease of more than 500 Hz after 180 min. Rinsing with buffer gave rise to an increased frequency shift, which is presumably due to enhanced lateral shear forces resulting in a facilitated rupture of vesicles on the surface. This indicates that, even after 180 min, the process of spreading is not completed. Under flow conditions, adsorption of vesicles could not be detected, even at high biotin-X-DHPE concentrations, which is probably due to shear stress under flow.

SFM imaging of BBSA and streptavidin monolayers on mica

A freshly cleaved mica sheet was first incubated with BBSA (1 mg/ml), rinsed with buffer and treated with streptavidin solution (0.1 mg/ml). After each incubation step, the surface was imaged by SFM both in buffer (contact mode) and in air (TappingMode) to obtain better resolution as a result of the sharper tip. Surface topography images after a 20-min incubation period with BBSA revealed high protein coverage exhibiting only few defects in the protein monolayer (Fig. 3 *A*). The thickness of the BBSA layer was determined by removing a narrow region of the protein layer in buffer (1 $\times 1$ μm^2) with the SFM tip at high load force and high scan rate followed by imaging at larger scale (5 $\times 5$ μm^2) with low load force. The height difference between the protein layer and the mica surface was calculated to be (2 ± 1) nm obtained from depth analysis, which is consistent with a BBSA monolayer. Incubation of the pretreated mica surface with streptavidin for 30 min results in a height increase of the protein layer (5–8 nm) and an increase in surface roughness due to the adsorption of streptavidin (Fig. 3 *B*). The roughness of the streptavidin layer (RMS: 0.7 nm) is significantly higher than that of the BBSA monolayer (RMS: 0.4 nm).

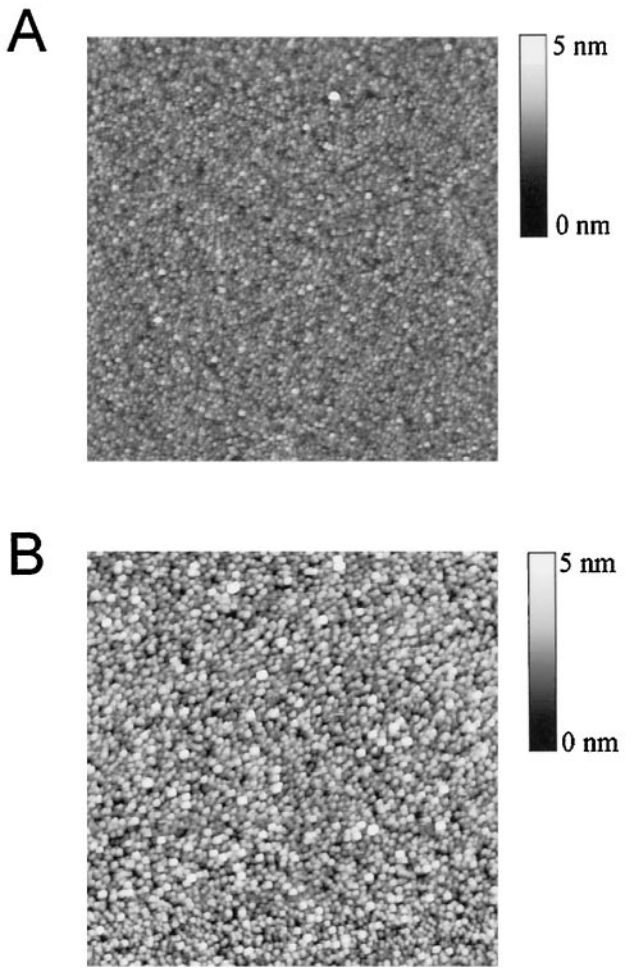

FIGURE 3 (*A*) Topographic SFM image (TappingMode) of a BBSA-covered mica sheet measured in air. Freshly cleaved mica was incubated in a 1 mg/ml BBSA solution for 20 min and rinsed with buffer to remove nonbound proteins before air drying. (*B*) Topographic SFM image (TappingMode) of a BBSA-covered mica sheet subsequently immersed in a 0.1 mg/ml streptavidin solution for 10 min. The surface was rinsed with buffer, and air dried. The image sizes are 2×2 μm^2.

SFM imaging of adherent liposomes

Incubating the streptavidin-treated mica surface with LUVs (1 mol% biotin-X-DHPE) at a lipid concentration of 0.1 mg/ml led to a large amount of aggregated liposomes (Fig. 4 *A*) with few individual vesicles. However, lower concentrations (0.01 mg/ml) resulted in well-separated individual liposomes (Fig. 4 *B*). In both cases, section analysis shows oblate spherical structures. Compared to the height of individual vesicles (~30–70 nm), aggregated liposomes are higher (~90–120 nm), indicating that the elastic properties of the ensemble is different. Although aggregated liposomes could be easily imaged even at higher load forces up to 1–2 nN without damaging, single vesicles were dragged and flatten at load forces higher than 1 nN. Individual liposomes are also more susceptible to lateral forces, as can be deduced from a slightly distorted profile. Besides lateral forces, indentation and adhesion also influence the vesicles' shape (see Scheme 1). Figure 5 shows the dependence of the liposomes' height on the load force resulting from adhesion and indentation. In our experiments, indentation of the liposomes was kept at a minimum by choosing the applied load force as low as possible (~100 pN).

The contour line of a vesicle monitored by SFM can be largely influenced by tip sample convolution, in particular, when the sample is high and steep. Reconstruction of a faithful image from a distorted one can be accomplished if the tip geometry is known. Figure 6 shows a center section of a liposome doped with 1 mol% biotin-X-DHPE adhered on a BBSA/streptavidin-covered mica surface. The load force was ~100 pN. The solid line is the result of applying

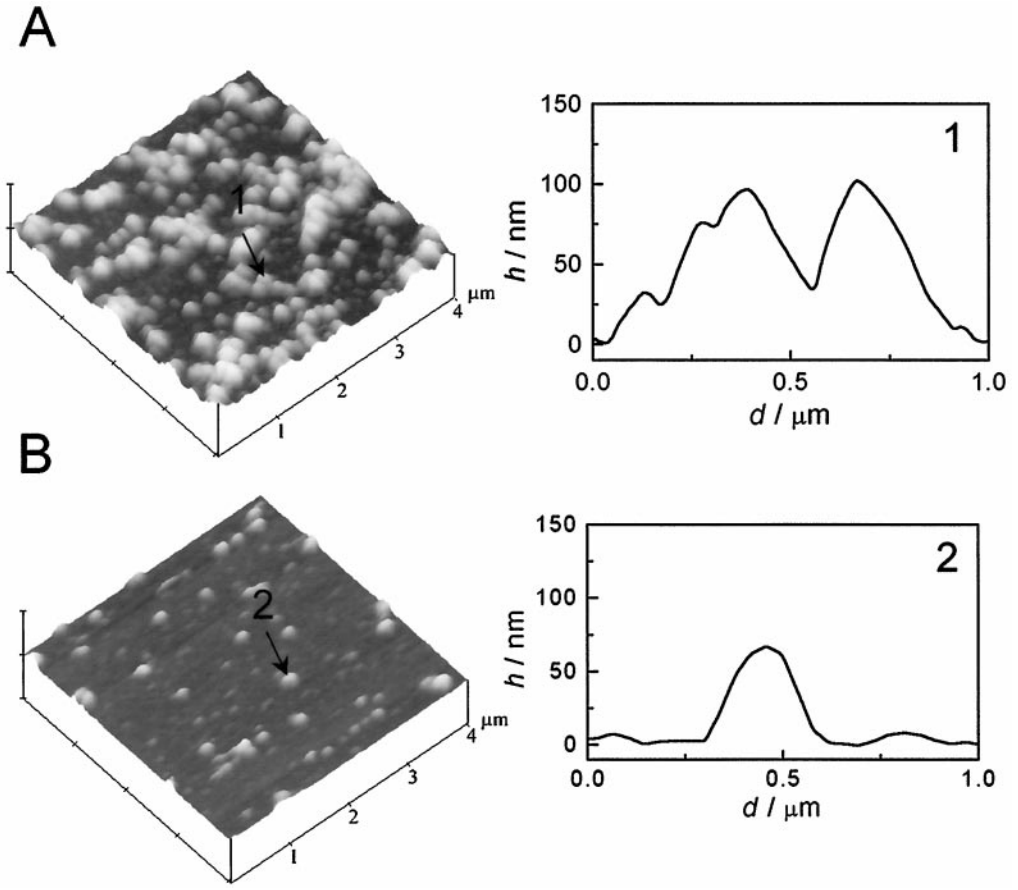

FIGURE 4 Three-dimensional topographic SFM images (contact mode in buffer) of LUVs adhered to a streptavidin layer. (*A*) The functionalized surface was incubated with LUVs doped with 1 mol% of biotin-X-DHPE at a concentration of 0.1 mg/ml for 20 min. Aggregates and single liposomes are discernible. The height profile of the marked liposome (*1*) is shown on the right hand side. (*B*) The streptavidin-coated surface was incubated with 1 mol% biotin-X-DHPE-doped vesicles at a concentration of 0.01 mg/ml for 20 min. Mainly individual liposomes are visualized by SFM. The height profile of a discrete liposome (*2*) is shown on the right hand side.

a deconvolution algorithm from Keller (1991) based on the Legendre transformation,

$$\mathrm{L}[s(x)] = \mathrm{L}[i(x')] + \mathrm{L}[t(\Delta x)], \qquad (1)$$

in which L is the common Legendre transform, $s(x)$ the true, $i(x')$ the reported contour line, and $t(\Delta x)$ the geometry of the tip. The transformed x axis can be obtained from $x = x' +$

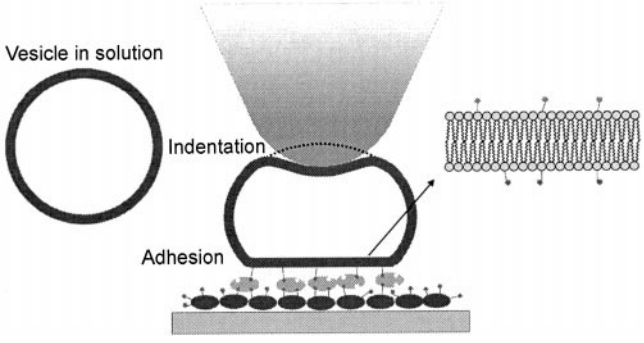

SCHEME 1 Schematic drawing depicting the shape of a biotinylated large unilamellar vesicle specifically adhered to a streptavidin layer by biotin–straptavidin interactions. In addition to the central displacement due to adhesion, the height of the vesicle is influenced by the indention of the tip.

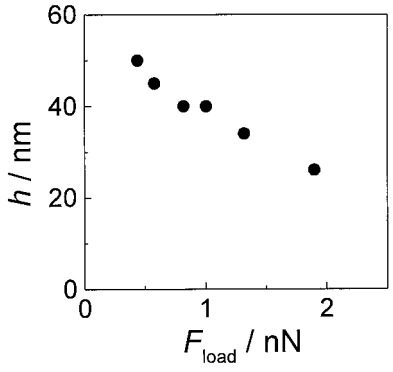

FIGURE 5 Vesicle height (h) versus tip load (F_{load}) curve of an individual large unilamellar vesicle doped with 1 mol% biotin-X-DHPE measured in buffer. The vesicle height decreases as a result of its increased indentation, and adhesion.

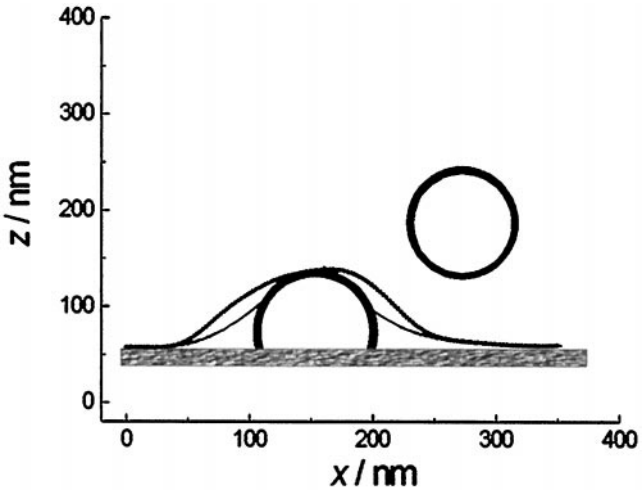

FIGURE 6 Contour line of an adhered DPPC vesicle (diameter 100 nm) doped with 1 mol% biotin-X-DHPE. The thin solid line is the line scan $i(x')$ obtained by SFM, whereas the thick solid line displays the deconvoluted contour line (parabolic tip shape, $R = 40$ nm). The true shape of the vesicle is presumably spherically capped.

Δx. The morphology of the vesicle can be roughly described as a capped sphere like a sessile drop. This is in accordance with theoretical work done by Seifert (1991), Seifert and Lipowski (1995), and Blockhuis and Sager (1999) dealing with the shape of adhered vesicles. The graph also demonstrates some of the limitation of imaging liposomes by SFM. The part of the liposome contour accessible by the tip is limited to ~10–30% of the total contour line length. Although only a limited part of the liposome can be visualized by SFM, no other technique is capable of imaging small vesicles in solution. Albersdörfer et al. (1997, 1998) successfully used reflection interference contrast microscopy to image the adhesion of giant vesicles ($R \approx 10$ μm) mediated by molecular recognition events at the solid/liposome interface.

Influence of biotin concentration on vesicle adhesion

The influence of biotin concentration on vesicle adhesion was investigated by SFM. When a vesicle adsorbs on the streptavidin layer, both nonspecific and specific interaction forces are involved in the adhesion process. While nonspecific interactions do not change significantly by altering the biotin-X-DHPE concentration, the increasing molecular recognition events between substrate and liposome induces a decreasing height of the liposomes. Topographic images of vesicles with different concentrations of biotinylated lipids adsorbed on a streptavidin layer are presented in Fig. 7 together with the corresponding section analysis. All images were obtained at ~100-pN load force using a lipid concentration of 0.01 mg/ml to obtain mainly individual liposomes. The most striking difference between the differently doped vesicles is the height. Vesicles doped with 1 mol% of biotin-X-DHPE (Fig. 4 *B*) show an oblate spherical structure with an average height of (50 ± 18) nm. Increasing the biotin concentration results in a considerable decrease in vesicle height. Although 10 mol% (Fig. 7 *A*) exhibits an average height of (36 ± 32) nm, 20 mol% (Fig. 7 *B*) leads to structures with a height of only (16 ± 10) nm. At 30 mol% biotin-X-DHPE (Fig. 7 *C*), the topography of the vesicles changed dramatically compared to vesicles with 1–10 mol%. The general appearance is flat rather than spherical or ellipsoidal. The average step height of (8 ± 2) nm is presumably indicative of spread bilayers. Notably, the bilayer structure exhibits a roughness, which is due to the BBSA/streptavidin layer, rendering an accurate measurement of the bilayer height difficult. The histogram shows a very narrow height distribution for 30 mol% biotin-X-DHPE (Fig. 8 *D*). Eighty-five percent of all liposomes are spread, forming lipid bilayers with typical heights of 5–8 nm, whereas 15% are higher with 10–12-nm thickness, which can be interpreted in terms of two bilayers stacked on top of each other. Intermediate structures are also discernible, composed of a double and a single bilayer. The number of spread bilayers decreases with decreasing percentage of biotinylated lipid. At a biotin-X-DHPE concentration of 20 mol%, only 37% spread bilayer is observable, whereas 30% exhibit a double bilayer structure and 43% are higher than 10 nm (Fig. 8 *B*). A very broad distribution was observed for vesicles doped with 1 mol% biotin (Fig. 8 *D*). The height ranges from 10 to 90 nm with a maximum at around 50 nm.

An experiment performed at higher lipid concentration (0.3 mg/ml) revealed that vesicles with 30 mol% biotin-X-DHPE spread to bilayers even at higher lipid concentrations. This is consistent with observations from Kalb et al. (1992), Plant et al. (1994), and our own experiments (Steinem et al., 1996). Because vesicles with 30 mol% biotin spread almost completely on the streptavidin layer, forming a planar bilayer with an almost round shape, we managed to calculate the vesicles' unperturbed diameter from the measured surface area using $A_b = 4\pi R_{ves}^2$, where A_b and R_{ves} are the area of the spread bilayer and the radius of the intact spherical vesicle, respectively. The obtained average value of A_b = (39,500 ± 15,170) nm^2 is equivalent to R_{ves} = (56 ± 10) nm in good accordance with results obtained from light-scattering experiments of free vesicles (40–60 nm).

Friction force analysis of the adhered vesicles

We performed friction force microscopy on samples with spread liposomes (30 mol% biotin-X-DHPE) to monitor material differences between the protein and the spread vesicles, which might be responsible for the observed frequency response of 550 Hz upon addition of liposomes doped with 30 mol% of biotinylated lipid (Fig. 9). The images show that the planar bilayers have a significant

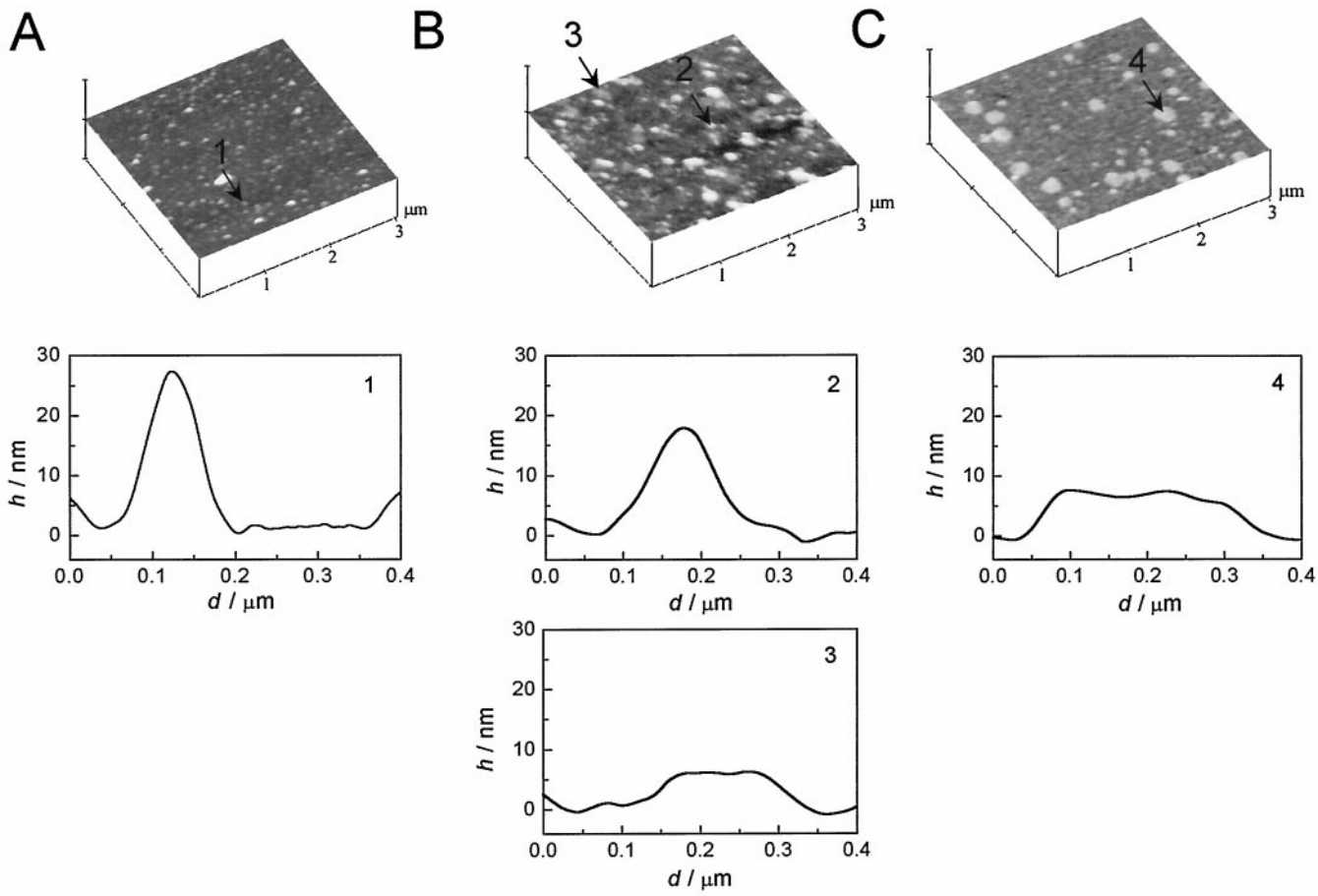

FIGURE 7 Three-dimensional topographic SFM images (contact mode in buffer) of large unilamellar DPPC vesicles doped with various biotin concentrations: (*A*) 10 mol%, (*B*) 20 mol%, (*C*) 30 mol%. The images were obtained at load forces of about 100 pN. Height profiles of individual liposomes (*arrows 1–4*) are shown below each image. (*A*) Liposomes carrying 10 mol% biotin-X-DHPE appear as deformed ellipsoids or spherical caps. (*B*) For the liposomes carrying 20 mol% biotin, both ruptured and intact vesicles can be observed. (*C*) At 30 mol%, almost all liposomes are spread, forming planar bilayers.

lower friction coefficient than does the protein layer. The observed contrast inversion between trace and retrace scans corroborates that contrast has its origin in friction and not topography. This difference in surface properties of the protein layer and the planar bilayer could be responsible for the observed frequency shift.

DISCUSSION

Adhesion of vesicles studied by QCM

Two major questions arise with respect to the obtained QCM results. Which effects influence the observed frequency shifts and, in particular, how does the morphology of the attached liposomes contribute to that effect? At first sight, it may be conceivable that a larger biotin-X-DHPE concentration leads to larger frequency shifts because more vesicles bind to the surface. A simple calculation reveals, however, that the overall biotin concentration for 1-mol%-doped liposomes is 4.5 μM in solution, which is more than sufficient to cover the entire avidin layer assuming a binding constant of 2×10^{10} M^{-1} for the streptavidin/biotin couple (Zhao and Reichert, 1992). (Compared to the binding constant in solution (10^{14}–10^{15} M^{-1}), the binding of streptavidin to a biotin on surface is, in general, much weaker due to steric hindrance.) However, taking into account that not every biotin is capable of binding to avidin due to steric hindrance and inaccessibility, the lowest limit of binding-capable species would be 3 nM. This arises from the calculation that one liposome composed of 150,000 lipids and doped with 1 mol% biotin contains ~1500 biotin molecules. Assuming that only one biotin-X-DHPE per liposome is capable of binding to avidin, an apparent biotin concentration of 3 nM (equivalent to a 98% surface coverage) has to be taken into account, which still does not explain the observed difference in frequency shift.

The aforementioned surface coverage was calculated assuming a Langmuir adsorption isotherm with a binding constant of 2×10^{10} M^{-1}. Besides, the overall number of

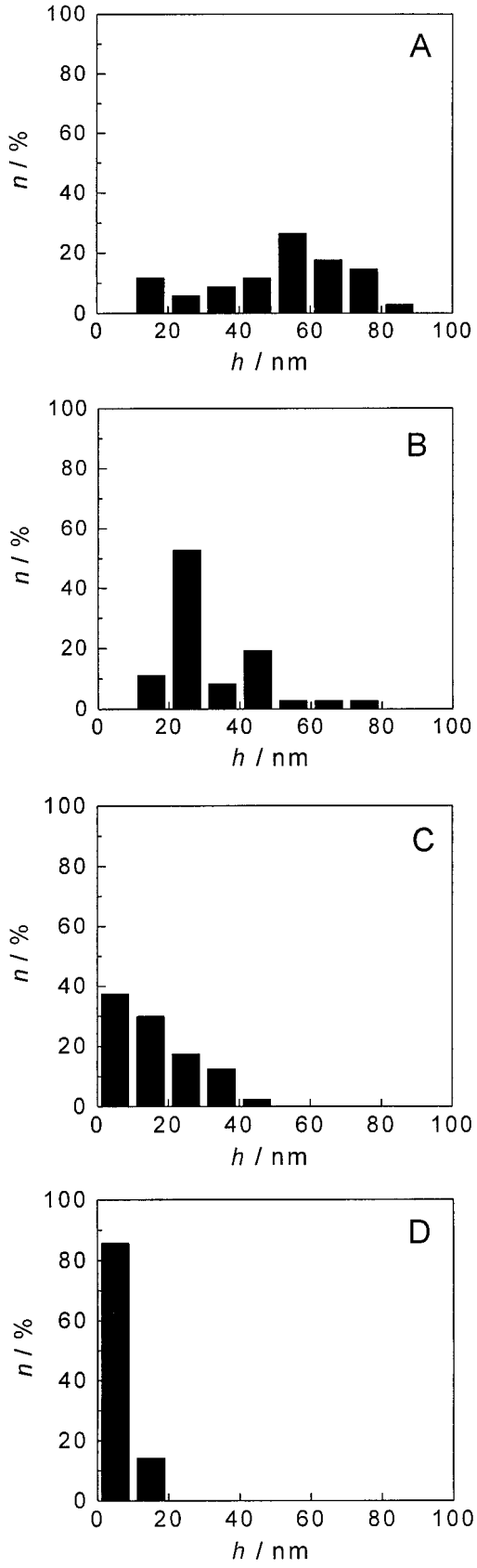

vesicles in solution exceeds the minimum number of vesicles necessary to cover the surface completely by a factor of 1000. Because, for 1 mol% biotinylated vesicles, a frequency change of 20 Hz was detected instead of 485 Hz (98% of the maximum frequency change of 500 Hz), we infer, in contrast to Yun et al. (1998), that the frequency decrease cannot be attributed to different amounts of bound vesicles to the surface or lack of vesicles in solution. From our point of view, the interpretation of Yun et al. does not apply in our case because of the high binding constant of the streptavidin/biotin couple as outlined above.

We hypothesized instead that the number of contacts to the surface, i.e., the overall contact area, causes the observed frequency shifts. The SFM studies, which verified that shape and contact area differ considerably with varying dopant concentrations, support this hypothesis. More biotin–streptavidin links result in a higher frequency decrease. The largest frequency shift was obtained from vesicles with 30 mol% forming mostly planar bilayers on the resonator surface. The idea that vesicle fusion to planar bilayers contributes considerably to the frequency shift was corroborated by Liebau et al. (1998), who could demonstrate that polymerized liposomes exhibited dramatically decreased frequency changes compared to nonpolymerized ones, which should be attributed to suppressed membrane fusion. In a similar fashion, vesicle fusion on hydrophobic surfaces leads to large frequency shifts ($>\Delta f = 230$ Hz at a resonant frequency of 5 MHz), considerably larger than expected using Sauerbrey's equation (Ohlsson et al., 1995; Janshoff et al., 1996), which can be interpreted in terms of dramatic changes in surface energies. Previously, Ward and coworkers could demonstrate that self-assembled monolayers of 11-mercaptoundecanoic acid immobilized on gold-coated quartz resonators (5 MHz) act with tremendous changes in resonant frequency upon pH changes, rendering the surface charged or uncharged (Wang et al., 1992). Shifts in frequency were as large as 1200 Hz resulting from a pH change from 5 to 8–9. Although not well understood, the considerable shift is most likely due to hydrodynamic effects, in which the connection between the water layer and the surface, as well as the water layer itself, changes dramatically depending on the charge of the surface. Based on these findings, we performed friction force measurements to find differences in material contrast between the protein layer and the planar membranes. The lateral force images clearly indicate that friction on the bilayer patches is less pronounced than on the protein layer due to different sur-

FIGURE 8 Height distribution histograms of large unilamellar vesicles doped with different amounts of biotin obtained from contact mode SFM figures imaged at load forces of about 100 pN. (*A*) 1 mol%, (*B*) 10 mol%, (*C*) 20 mol%, (*D*) 30 mol%. Forty vesicles were analyzed for one histogram. The average height of the vesicles decreases considerably with increasing amount of biotin.

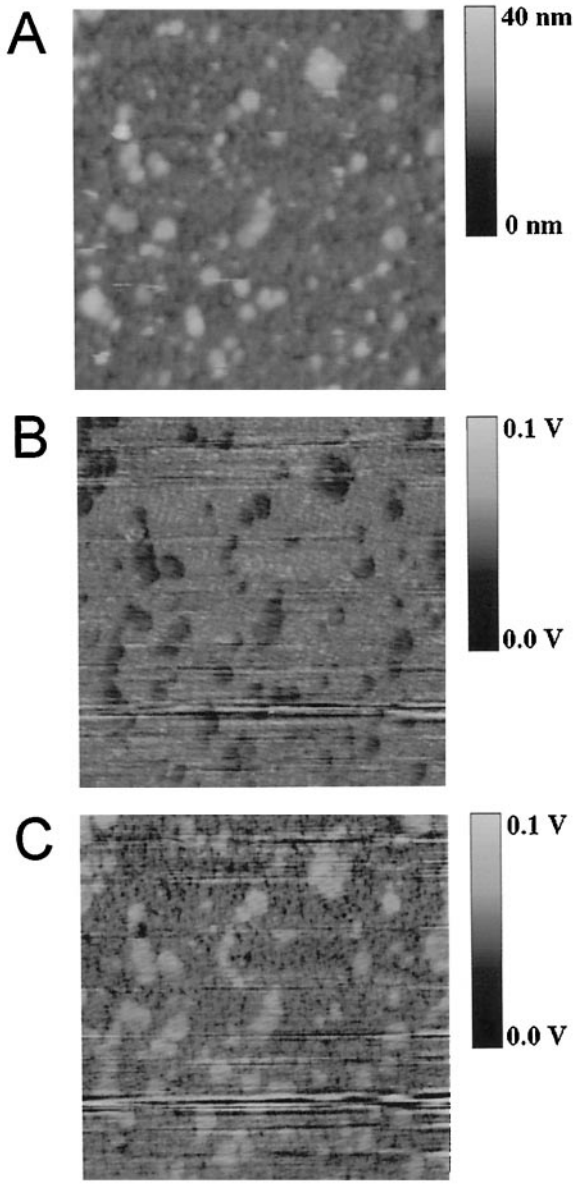

FIGURE 9 Lateral force SFM images of spread liposomes composed of 70 mol% DPPC, and 30 mol% biotin-X-DHPE: (*A*) Topography, (*B*) forward-scan direction (trace), (*C*) backward scan direction (retrace). The observed contrast inversion between forward and backward scan direction confirms that the contrast is not due to topography but to material differences. The protein layer exhibits a higher friction coefficient than does the planar bilayer, indicating more adhesive interaction with the tip.

face properties leading to a modified interaction with the SFM-tip. Although this experiment does not give direct information about the origin of the high frequency shift, it gives a first clue about possible reasons involving surface properties. More systematic experiments are currently on the way to seek a more general understanding of the phenomena, which are contributing to the frequency shift observed by deposition of biomaterials.

Besides thermodynamic considerations, the kinetics of vesicle adhesion exhibits some interesting peculiarities, which should be addressed. Generally, kinetics of the liposome adsorption can be explained by mass transport. Sedimentation of liposomes onto the resonator surface can be neglected because it would take $\sim t_{max} = 1000$ h for a liposome (viscosity of water $\eta^{20}_{H_2O} = 1.002 \times 10^{-2}$ g/(cm·s), density of water $\rho_{H_2O} = 0.99823$ g/cm^3, radius of the liposome $R = 50$ nm, density of the liposome (Goormaghtigh and Scarborough, 1986) $\rho_{vesicle} = 1.047$ g/cm^3) to travel the distance of $h = 10$ mm in water just by sedimentation:

$$t_{max} = \frac{9}{2}\frac{\eta_{H_2O}}{g(\rho_{vesicle} - \rho_{H_2O})R^2}h. \quad (2)$$

Although sedimentation does not contribute much to the adsorption kinetics of small vesicles, it has a considerable influence on the mass transport to the surface of seeded cells and giant liposomes in an unstirred solution. However, it could be demonstrated that adhesion kinetics of cells is practically independent of sedimentation because it is too fast (Wegener et al., 1998).

The observed time course of the frequency shift can be attributed to planar diffusion in an unstirred solution. At high liposome concentrations, i.e., the Langmuir adsorption isotherm has leveled off, diffusion to the surface can be described by (Delahay and Trachtenberg, 1957):

$$\Delta f = -2\frac{\Delta f_{max}}{\Gamma_{R,O}}c_{L,O}\sqrt{\frac{D}{\pi}t}. \quad (3)$$

D is the diffusion constant, $c_{L,0}$ the concentration of the ligand (liposome) in solution, Γ_{RO} the highest possible surface concentration, and Δf_{max} the maximum frequency shift. Assuming a diffusion constant D for the liposomes in buffer of 4.29×10^{-8} cm^2/s, by using the Stoke–Einstein relationship, a vesicle concentration $c_{L,0}$ of 3 nM and a binding constant for the biotin-lipid/streptavidin couple of $K_a = 2 \times 10^{10}$ M^{-1}, Eq. 3 reveals a time course, which is in the same time scale as the experimental data. Evaluation of the kinetics by taking multiple binding sites into account is cumbersome, and the development of a more sophisticated diffusion model is part of the current research.

Another aspect to consider with respect to adsorption kinetics is the lateral diffusion of receptor lipids within the bilayer, which occurs on a time scale important for the observed frequency course. Biotin receptors move from the opposite side of the liposome to a surface-bound streptavidin resulting in a locally increased number of contacts. Albersdörfer et al. (1997) demonstrated that lateral diffusion plays a key role in the adhesion of giant liposomes. Using $t = x^2/4D$ with $D = 0.5 \times 10^{-10}$ cm^2/s for DPPC below the main phase transition temperature, lateral diffusion on the length scale of $x = 100$ nm is rather fast ($t =$

0.25 s), which renders lateral diffusion a minor contribution to the adsorption kinetics.

Although diffusion is presumably responsible for the observed time course of the frequency response, what causes the delayed frequency response at the beginning of the experiment has to be elucidated. The sigmoidal time trace at the beginning may be due to a cooperative binding induced by surface-enhanced vesicle fusion. Seifert and Lipowski (1995) pointed out that adhesion favors fusion of liposomes. Consequently, the liposome size increases, leading to a larger contact area, thus inducing a larger signal. Furthermore, rupture to planar bilayers is favored because edge tension of the resulting open disc is smaller compared to individually spread liposomes.

To some extent, the time trace resembles the kinetics of cell adhesion (MDCK II) in the presence of different concentrations of focal contact-inhibiting peptides (RGD) (Wegener et al., 1998). The addition of different concentrations of the RGD peptides reduces the number of binding sites of the cell, which leads to slower adhesion kinetics. This striking similarity, together with the similar maximum frequency shifts between cell and vesicle adhesion, support the idea that receptor-doped vesicles are useful model systems for the investigation of cell adhesion phenomena. Thus, we hypothesize that the number of contacts to the surface causes the different frequency shifts because it alters the contact area and shape of the vesicles.

SFM-imaging of adherent liposomes

Imaging of small liposomes (~100 nm) in situ is a challenge, which can solely be accomplished by scanning probe microscopy techniques. Only a few studies on vesicle topography in buffer solution are available. This is mainly due to the high lateral forces that occur during imaging, resulting in unstable scanning, dragging, and disruption of the liposomes (Benoit et al., 1997; Shibata-Seki et al., 1996). The lateral force applied on the liposome is a function of vertical load, aspect ratio, tilt angle of the cantilever, and the friction coefficient between the tip and the object. The lateral force in constant-height mode is extremely sensitive to the angle between tip and object (Benoit et al., 1997). In fact, the lateral force exceeds the load force, i.e., the vertical applied force in most cases. For instance, using an angle α of 30° between tip and sample, a friction coefficient μ of 0.4, a normalized cantilever stiffness $d/(kl^2)$ of 0.01 N^{-1}, and a vertical load force F_{vertical} of 100 pN, a lateral force F_{lateral} of about 1.1 nN results by solving Eq. 4 numerically (Benoit et al., 1997):

$$\frac{F_{\text{lateral}}}{F_{\text{vertical}}}\tan\left[\alpha+\arctan\left(F_{\text{lateral}}\frac{d}{kl^2}\right)\right]+\frac{\mu\cos[\alpha+\arctan(F_{\text{lateral}}(d/kl^2))]}{\mu-\alpha+\arctan(F_{\text{lateral}}(d/kl^2))}=1. \quad (4)$$

Depending on the feedback mode and scan direction, the situation can lead to a considerable distortion of the image. Besides lateral forces, indentation arising from high vertical load forces can be tremendous. Indentation of soft structures leads to severe difficulties determining vertical dimensions. For instance, Müller et al. (1997a) observed, that lipid vesicles form bilayer structures on mica under a load force exceeding 100 pN using standard oxide-sharpened tips (Digital Instruments). However, Shibata-Seki et al. (1996) found, that aggregated vesicles are more resistant to vertical and lateral load forces than are isolated vesicles. Adhesion also has to be taken into account. Load forces applied by the SFM tip lead to enhanced adhesion forces and therefore larger contact areas, resulting in a diminished height of the structures (Seifert and Lipowski, 1995; Seifert, 1991). Deformation due to adhesion can be of the same magnitude as indentation. Scheme 1 shows the two main contributions—indentation and adhesion—influencing the morphology of the attached liposomes. Because indentation and adhesion are both influenced by the tip load, they cannot be treated separately. However, separate treatment can be helpful to obtain a rough idea about the order of magnitude these effects affect the SFM images. To get an approximation about the indentation caused by the tip-neglecting adhesion on the one hand, one can apply the theory of elastic body deformation as developed by Hertz (Landau and Lifschitz, 1965). An applied load force of $F = 100$ pN on an elastic sphere (Young modulus $E_{\text{ves}} = 2 \times 10^5$ Pa, Poisson ratio $\nu_{\text{ves}} = 0.5$, $R_{\text{ves}} = 50$ nm) from a tip ($E_{\text{tip}} = \infty$, $R_{\text{tip}} = 50$ nm) (Laney et al., 1997) would cause an indentation of the elastic body of $\delta = 7$ nm using

$$\delta = \left(\frac{RF}{K}\right)^{2/3}\frac{1}{R}, \quad (5)$$

with

$$K \cong \frac{4}{3\pi}\cdot\left(\frac{1-\nu_{ves}^2}{\pi E_{\text{ves}}}\right) \quad \text{and} \quad R = \frac{R_{\text{ves}}R_{\text{tip}}}{R_{\text{ves}}+R_{\text{tip}}}. \quad (6)$$

Neglecting the tip indentation on the other hand, the deformation of a liposome due to adhesion under load can be calculated according to the theory developed by Johnson et al. (1971) and Israelachvili (1994). The same liposome would deform by $\delta = 8.5$ nm due to a load force of $F = 100$ pN, assuming an adhesion energy W between the elastic body and the planar surface of 5×10^{-4} J/m^2 according to

$$\delta = \frac{((R/K)\{F+3\pi RW+[6\pi RWF+(3\pi RW)^2]^{0.5}\})^{2/3}}{R}\times\left[1-\frac{2}{3}\frac{(6\pi R^2W/K)^{0.5}}{((R/K)\{F+3\pi RW+[6\pi RWF+(3\pi RW)^2]^{0.5}\})^{0.5}}\right]. \quad (7)$$

It should be pointed out that the above considerations are only rough estimations, which do not use the general theory

of shells. For a more sophisticated and detailed analysis of vesicle adhesion, please refer to the comprehensive work of Seifert and Lipowski (1995).

The observed shape and rupture point of the adhered liposomes can also be predicted theoretically. The balance between cost in curvature energy and gain in adhesion energy determines the shape of the bound vesicle. The liposomes' shape can be obtained by solving the variational problem, i.e., the corresponding Euler–Lagrange equations (Seifert and Lipowski, 1995). Larger liposomes require a smaller minimal adhesion energy W_a to adhere on a given substrate. The contact area vanishes for $W = W_a$ with

$$W_a = \frac{2\kappa}{R^2}, \tag{8}$$

in which R is the radius of the unperturbed vesicle and κ denotes the Helfrich bending rigidity of the liposome. Adhesion induces fusion because the gain in energy of two bound vesicles fusing is larger than that of two free vesicles. As the size of the fusing liposome increases, its shape resembles that of a pancake. Adherent liposomes eventually rupture if the elastic tension exceeds the threshold for lysis. According to Seifert and Lipowski, lysis typically occurs at an upper limit of $(A - A_0)/A_0 \cong 0.03$. A_0 denotes the surface area before and A after stretching. Adhesion-induced stretching is usually in the order of $(A - A_0)/A_0 \cong W/k$, where k is the area compressibility modulus of the bilayer and is in the order of 10^2 mJ/m^2. After rupture, the conformation of the planar bilayer is that of an open disc. Due to the edge tension occurring along the boundary, bilayers fuse to larger assemblies, resulting in high-resistant solid-supported membranes. A simple estimation suggests that apparently not all streptavidin biotin-X-DHPE pairs have been formed. Assuming a binding constant K of 2×10^{10} l/mol ($\Delta G = -58.8$ kJ/mol), the adhesion energy can be estimated assuming that all biotins are bound to streptavidin. For a liposome containing 30 mol% biotin-X-DHPE, the adhesion energy would be 99 mJ/m^2, which exceeds the limit of 2.1 mJ/m^2 at which a liposome starts to form planar bilayers on the surface.

CONCLUSIONS

In this study, we addressed the question of how the morphology of the attached liposomes influence the frequency response of the QCM, and we were interested in the spreading behavior of vesicles to form planar bilayers. This latter issue is particularly important for the rising number of biosensor applications using solid-supported membranes as biocompatible surfaces for integration and attachment of bioactive components. Specific adsorption of biotinylated liposomes was followed by shear wave resonator measurements, whereas the microscopic details were investigated by SFM. Increasing the amount of biotinylated lipids gives rise to an increase in frequency shift, which is apparently due to the establishment of an increasing amount of biotin–streptavidin linkages. Therefore, the contact area between vesicles and protein layer increases, which could be confirmed by shape analysis performed by SFM measurements. If the amount of biotinylated lipids exceeds 30 mol%, rupture of the liposome occurs, forming planar lipid bilayers that are firmly attached to the surface. These results clearly indicate that the formation of streptavidin–biotin bonds is responsible for the observed frequency shift by reducing the distance between the attached liposomal membrane and the protein layer. Changes in surface properties by depositing planar bilayers alter the hydrodynamic behavior of the water layer on top of the membrane, thus resulting in tremendous frequency shifts. Interestingly, the results are similar to those of a QCM-study of different mammalian cells attaching to quartz resonators. Because adhesion kinetics and maximum frequency shifts of cells and functionalized liposomes show similar results, vesicles seemed to be good model systems to study cell adhesion by shear wave resonator measurements.

The work has been financially supported by the habilitation program of the Deutsche Forschungsgemeinschaft (A.J.), a Lise-Meitner fellowship (C.S.) and Ministero per l'Università e la Ricerca Scientifica e Tecnologica (B.P.).

We thank our colleagues Joachim Wegener, Christian Röthig, Li-Feng Chi, and Steven Lenhert for valuable input.

REFERENCES

Albersdörfer, A., R. Bruinsma, and E. Sackmann. 1998. Force spectroscopy on adhesive vesicles. *Europhys. Lett.* 42:227–231.

Albersdörfer, A., T. Feder, and E. Sackmann. 1997. Adhesion-induced domain formation by interplay of long-range repulsion and short-range attraction force: a model membrane study. *Biophys. J.* 73:245–257.

Benoit, M., T. Holstein, and H. E. Gaub. 1997. Lateral forces in AFM imaging and immobilization of cells and organelles. *Eur. Biophys. J.* 26:283–290.

Binnig, G., C. F. Quate, and C. Gerber. 1986. Atomic force microscope. *Phys. Rev. Lett.* 56:930–933.

Blokhuis, E. M., and F. C. Sager. 1999. Helfrich free energy for aggregation and adhesion. *J. Chem. Phys.* 110:3148–3152.

Bongrand, P. 1995. Adhesion of Cells. Elsevier, Amsterdam, The Netherlands.

Buttry, D. A., and M. D. Ward. 1992. Measurement of interfacial processes at electrode surfaces with the electrochemical quartz crystal microbalance. *Chem. Rev.* 92:1355–1379.

Cooper, S. L., C. H. Bamford, and T. Tsuruta. 1995. Polymer Biomaterials: In Solution, as Interfaces and as Solids, VSP Zeist, Utrecht, The Netherlands.

Delahay, B. P., and I. Trachtenberg. 1957. Adsorption kinetics and electrode processes. *J. Am. Chem. Soc.* 79:2355–2362.

Gallez, D. 1994. Non-linear stability analysis for animal cell adhesion to solid support. *Colloids Surf. B.* 2:273–280.

Goormaghtigh, E., and G. A. Scarborough. 1986. Density based separation of liposomes by glycerol gradient centrifugation. *Anal. Biochem.* 159: 122–131.

Hutter, J. L., and J. Bechhoefer. 1993. Calibration of atomic-force microscope tips. *Rev. Sci. Instrum.* 64:1868–1873.

Israelachvili, J. N. 1994. Intermolecular and Surface Forces. Academic Press, San Diego, CA.

Janshoff, A., C. Steinem, M. Sieber, and H. J. Galla. 1996. Specific binding of peanut agglutinin to G_{M1}-doped solid supported lipid bilayers investigated by shear wave resonator measurements. *Eur. Biophys. J.* 25: 105–113.

Johnson, K. L., K. Kendall, and A. D. Roberts. 1971. Surface energy and the contact of elastic solids. *Proc. R. Soc. Lond. Ser. A.* 324:301–313.

Kalb, E., S. Frey, and L. K. Tamm. 1992. Formation of supported planar bilayers by fusion of vesicles to supported phospholipid monolayers. *Biochim. Biophys. Acta.* 1103:307–316.

Keller, D. 1991. Reconstruction of STM and AFM images distorted by finite-size tips. *Surf. Sci.* 253:353–364.

Landau, L. D., and E. M. Lifschitz. 1965. Elastizitätstheorie. Akademie-Verlag, Berlin, Germany.

Laney, D. E., R. A. Garcia, S. M. Parsons, and H. G. Hansma. 1997. Changes in the elastic properties of cholinergic synaptic vesicles as measured by atomic force microscopy. *Biophys. J.* 72:806–813.

Liebau, M., G. Bendas, U. Rothe, and R. H. H. Neubert. 1998. Adhesive interactions of liposomes with supported planar bilayers on QCM as a new adhesion model. *Sens. Actuators B.* 47:239–245.

Müller, D. J., M. Amrein, and A. Engel. 1997a. Adsorption of biological molecules to a solid support for scanning probe microscopy. *J. Struct. Biol.* 119:172–188.

Müller, D. J., C. A. Schoenenberger, F. Schabert, and A. Engel. 1997b. Structural changes in native membrane proteins monitored at subnanometer resolution with the atomic force microscope: a review. *J. Struct. Biol.* 119:149–157.

Ohlsson, P.-A., T. Tjaernhage, E. Herbai, S. Loefas, and G. Puu. 1995. Liposome and proteoliposome fusion onto solid substrates, studied using atomic force microscopy, quartz crystal microbalance and surface plasmon resonance. Biological activities of incorporated components. *Bioelectrochem. Bioenerg.* 38:137–148.

Pignataro, B., E. Conte, A. Scandurra, and G. Marletta. 1997. Improved cell adhesion to ion beam polymer surfaces. *Biomaterials.* 18: 1461–1470.

Plant, A. L., M. Gueguetchkeri, and W. Yap. 1994. Supported phospholipid/alkanethiol biomimetic membranes: insulating properties. *Biophys. J.* 67:1126–1133.

Ruardy, T. G., H. C. van der Mei, H. J. Busscher, and J. M. Schakenraad. 1997. Preparation and characterization of chemical gradient surfaces and their application for the study of cellular interaction phenomena. *Surface Science Rep.* 29:1–30.

Sauerbrey, G. 1959. Verwendung von Schwingquarzen zur Waegung duenner Schichten und zur Mikrowaegung. *Z. Phys.* 155:206–222.

Schabert, F., and A. Engel. 1995. Atomic Force Microscopy of Biological Membranes: Current Possibilities and Prospects. Kluwer, Academic Publishers, Amsterdam, The Netherlands.

Seifert, U. 1991. Adhesion of vesicles in two dimensions. *Phys. Rev. A.* 43:6803–6814.

Seifert, U., and R. Lipowski. 1995. Morphology of Vesicles. Elsevier, Amsterdam, The Netherlands.

Shao, Z., and J. Yang. 1995. Progress in high resolution atomic force microscopy in biology. *Quater. Rev. Biophys.* 28:195–251.

Shibata-Seki, T., J. Masai, T. Tagawa, T. Sorin, and S. Kondo. 1996. In-situ atomic force microscopy study of lipid vesicles adsorbed on a substrate. *Thin Solid Films.* 273:297–303.

Steinem, C., A. Janshoff, and H.-J. Galla. 1998. Evidence for multilayer formation of melittin on solid-supported phospholipid membranes by shear wave resonator measurements. *Chem. Phys. Lipids.* 95:95–104.

Steinem, C., A. Janshoff, H.-J. Galla, and M. Sieber. 1997. Impedance analysis of the ion transport through gramicidin channels incorporated in solid supported lipid bilayers. *Bioelectrochem. Bioenerg.* 42:213–220.

Steinem, C., A. Janshoff, W.-P. Ulrich, M. Sieber, and H.-J. Galla. 1996. Impedance analysis of supported lipid bilayer membranes: a scrutiny of different preparation techniques. *Biochim. Biophys. Acta.* 1279: 169–180.

Terrettaz, S., T. Stora, C. Duschl, and H. Vogel. 1993. Protein binding to supported lipid membranes: investigation of the cholera toxin-ganglioside interaction by simultaneous impedance spectroscopy and surface plasmon resonance. *Langmuir.* 9:1361–1369.

Wang, J., L. M. Frostmann, and M. D. Ward. 1992. Self-assembled thiol monolayers with carboxylic acid functionality: measuring pH-dependent phase transitions with the quartz crystal microbalance. *J. Phys. Chem.* 96:5226–5228.

Wegener, J., A. Janshoff, and H. J. Galla. 1998. Cell adhesion monitoring using a quartz crystal microbalance: comparative analysis of different mammalian cell lines. *Eur. Biophys. J.* 28:26–37.

Yang, M., and M. Thompson. 1993a. Multiple chemical information from the thickness shear mode acoustic wave sensor in the liquid phase. *Anal. Chem.* 65:1158–1168.

Yang, M., and M. Thompson. 1993b. Surface morphology and the response of the thickness-shear mode acoustic wave sensor in liquids. *Langmuir.* 9:1900–1904.

Yun, K., E. Kobatake, T. Haruyama, M. L. Laukkanen, K. Keinanen, and M. Aizawa. 1998. Use of a quartz crystal microbalance to monitor immunoliposome–antigen interaction. *Anal. Chem.* 70:260–264.

Zhao, S., and W. M. Reichert. 1992. Influence of biotin lipid surface density and accessibility on avidin binding to the tip of an optical fiber sensor. *Langmuir.* 8:2785–2791.